MOLECULAR AND CELLULAR BIOLOGY, May 2009, p. 2794–2803 Vol. 29, No. 10
0270-7306/09/$08.00+0 doi:10.1128/MCB.01633-08

Thoc1 Deficiency Compromises Gene Expression Necessary for Normal Testis Development in the Mouse▽§

Xiaoling Wang,[1]† Meenalakshmi Chinnam,[1] Jianmin Wang,[2] Yanqing Wang,[1] Xiaojing Zhang,[1] Edyta Marcon,[3] Peter Moens,[3] and David W. Goodrich[1]*

Department of Pharmacology & Therapeutics[1] and Department of Cancer Genetics,[2] Roswell Park Cancer Institute, Elm & Carlton Streets, Buffalo, New York 14263, and Department of Biology, York University, Toronto, Ontario M3J 1P3, Canada[3]

Received 20 October 2008/Returned for modification 14 December 2008/Accepted 8 March 2009

Accumulating evidence suggests that regulation of RNA processing through an RNP-driven mechanism is important for coordinated gene expression. This hypothesis predicts that defects in RNP biogenesis will adversely affect the elaboration of specific gene expression programs. To explore the role of RNP biogenesis on mammalian development, we have characterized the phenotype of mice hypomorphic for *Thoc1*. *Thoc1* encodes an essential component of the evolutionarily conserved TREX complex. TREX accompanies the elongating RNA polymerase II and facilitates RNP assembly and recruitment of RNA processing factors. Hypomorphic *Thoc1* mice are viable despite significantly reduced *Thoc1* expression in the tissues examined. While most tissues of *Thoc1*-deficient mice appear to develop and function normally, gametogenesis is severely compromised. Male infertility is associated with a loss in spermatocyte viability and abnormal endocrine signaling. We suggest that loss of spermatocyte viability is a consequence of defects in the expression of genes required for normal differentiation of cell types within the testes. A number of the genes affected appear to be direct targets for regulation by *Thoc1*. These findings support the notion that *Thoc1*-mediated RNP assembly contributes to the coordinated expression of genes necessary for normal differentiation and development in vivo.

The coordinated expression of functionally related genes is required for normal cellular differentiation, development, homeostasis, and responses to environmental stimuli. The combinatorial action of sequence-specific DNA binding transcription factors at promoters provides the foundation for coordinated gene expression. However, even tissue-restricted gene expression is fraught with considerable stochastic noise (2, 28, 39). Furthermore, transcription may be coordinately initiated at genes that vary considerably in length, exon-intron structure, and primary nucleotide sequence. Thus, the speeds and efficiencies of transcriptional elongation, RNA processing, nuclear export, and protein translation may differ considerably from gene to gene. Accumulating evidence indicates that these postinitiation events may be regulated through a ribonucleoprotein particle (RNP)-driven mechanism (25). It has been suggested that dynamic RNP formation may segregate pre-mRNAs into "RNA regulons" to ensure coordinated protein production from functionally related genes (13). Disruption of this regulation is predicted to compromise the elaboration of specific gene expression programs, some of which may affect cellular differentiation and development. In vivo evidence in support of this prediction is lacking, particularly in higher eukaryotes.

The evolutionarily conserved TREX protein complex contributes to RNP biogenesis and RNA processing. The metazoan *Thoc1* gene and its *Saccharomyces cerevisiae* functional orthologue *HPR1* (both orthologues are subsequently referred to as *Thoc1* for simplicity) encode proteins that are essential components of the TREX complex (35). *Thoc1* protein (pThoc1) physically associates with the elongating RNA polymerase II (POLII) complex (4, 18) and recruits RNA processing and export factors to the nascent pre-mRNA (18, 35, 40). Depletion of pThoc1 permits the abnormal accumulation of RNA:DNA hybrids between the nascent RNA and the DNA template, underscoring the requirement for pThoc1 in RNP biogenesis (12, 18). The RNP assembly defect in *Thoc1*-deficient cells adversely affects transcriptional elongation (5, 6, 18, 30) as well as subsequent steps in RNA processing, including nuclear export (27, 35, 40).

Depletion of pThoc1 retards the expression of some but not all genes (18, 27, 35). It is currently unknown how genes subject to regulation by pThoc1 and TREX are specified. TREX can be assembled on model pre-mRNAs during in vitro transcription and splicing reactions. In vitro assembly is dependent on the RNA cap and splicing (7, 21, 23). However, pThoc1 itself can associate with at least some model pre-mRNAs independent of other TREX proteins and in the absence of splicing or the RNA cap binding protein CBP80 (23). *Thoc1* protein also appears to associate more intimately with the DNA template than do other TREX proteins (1). These observations suggest that pThoc1 may function early in RNP biogenesis. As pThoc1 has been documented to occupy promoter proximal regions of genes (14, 18), specification for regulation by pThoc1 may occur relatively early in the transcription cycle, possibly through interaction with transcription factors. Consistent with

* Corresponding author. Mailing address: Department of Pharmacology & Therapeutics, Roswell Park Cancer Institute, Elm & Carlton Streets, Buffalo, NY 14263. Phone: (716) 845-4506. Fax: (716) 845-8857. E-mail: david.goodrich@roswellpark.org.

† Present address: Box 0738, 533 Parnassus Ave., UC Hall, University of California, San Francisco, San Francisco, CA 94143-0738.

§ Supplemental material for this article may be found at http://mcb.asm.org/.

▽ Published ahead of print on 23 March 2009.

this view, pThoc1 physically interacts with the Rb1 tumor suppressor gene product (9), a known regulator of transcription initiation.

Yeasts completely lacking *Thoc1* are viable but are temperature sensitive for growth (10) and have reduced replicative potential (22). Loss of *Thoc1* in the mouse causes peri-implantation embryonic lethality with a marked loss of inner-cell-mass viability (36). *Thoc1* depletion also adversely affects the viability of several cancer cell lines cultured in vitro (11, 17). Interestingly, while oncogene-transformed cells are sensitive to pThoc1 depletion, isogenic normal cells appear to be relatively insensitive to reduced levels of pThoc1. This suggests that *Thoc1* may not be essential for the viability of all mammalian cell types. Due to the early embryonic lethality of *Thoc1* knockout mice, however, it has not been possible to test this possibility and evaluate whether *Thoc1* deficiency and associated defects in RNP biogenesis affect specific gene expression programs in the developing mouse and adult mouse.

To overcome this limitation, we have constructed a hypomorphic allele of *Thoc1* (*Thoc1*^{H}) in the mouse (37). Mice homozygous for the hypomorphic allele survive to term and are viable, despite reduced levels of pThoc1 in tissues where it has been examined. *Thoc1*$^{H/H}$ mice are proportionally smaller than their wild-type littermates but otherwise appear and behave normally. Thus, the differentiation, function, and homeostasis of most cell types appear to tolerate reduced levels of pThoc1. However, the fertility of both male and female hypomorphic *Thoc1* mice is severely diminished. Here, we characterize testis development and spermatogenesis in hypomorphic *Thoc1* mice. Our results suggest that pThoc1 contributes to the elaboration of specific gene expression programs necessary for cellular differentiation within the testes. These observations support the hypothesis that RNP biogenesis contributes to the regulation of coordinated gene expression during development.

MATERIALS AND METHODS

Hypomorphic *Thoc1* mice. The generation and PCR genotyping of the hypomorphic murine *Thoc1* allele have been previously described (37). Mice were maintained on a mixed C57BL/6 × 129SvJ genetic background. Homozygous *Thoc1*$^{H/H}$ mice for analysis were generated by an intercross of *Thoc1*$^{H/+}$ mice.

To induce superovulation, wild-type C57BL/6J female mice were given an intraperitoneal injection of pregnant mare's serum gonadotropin (5 IU per animal; Sigma-Aldrich, St. Louis, MO), followed 47 h later by an injection of human chorionic gonadotropin (5 IU per animal; Sigma-Aldrich, St. Louis, MO). Treated females were bred with *Thoc1*$^{H/H}$ or wild-type littermate control males, and the morning of detection of the vaginal plug was designated as presumptive embryonic day 0.5 (E0.5). Preimplantation embryos (E1.5 to E4.0) for analysis were collected by flushing the oviduct or uterus with HEPES-buffered medium 2 (M2; Sigma-Aldrich, St. Louis, MO). All animal work has been approved by the RPCI Institutional Animal Care and Use Committee and meets federal guidelines.

Hormone measurements. Blood samples from mice of 3 to 4 months of age were collected by cardiac puncture under anesthesia. Serum samples were separated by centrifugation at 4,000 rpm for 20 min at 4°C and stored at −20°C until assayed. Analysis of testosterone, growth hormone, luteinizing hormone, and insulin-like growth factor 1 was performed at the Vanderbilt Hormone Assay & Analytical Services Core, using a double-antibody radioimmunoassay.

Histology. Tissue for routine analysis of histology was fixed in 10% phosphate-buffered formalin or Bouin's fixative and then embedded in paraffin, sectioned (5 μm), and stained with hematoxylin and eosin by standard methods.

Immunostaining. Paraffin sections were cut at 5 μm, placed on charged slides, and dried in a 60°C oven for 1 h. Slides were deparaffinized in three changes of xylene and rehydrated using graded alcohols. Endogenous peroxidase was quenched with aqueous 3% H_2O_2 for 10 min and washed with PBST (10 mM sodium phosphate, 2 mM potassium phosphate [pH 7.4], 140 mM NaCl, 3 mM KCl, 0.1% [vol/vol] Tween 20). Antigen retrieval was performed in a microwave for 10 min in pH 6.0 citrate buffer and was followed by a 15-min cool down and PBST wash. Slides were blocked with 0.03% casein in PBST for 30 min and then incubated with primary antibody for 1 hour. An isotype-matched control antibody was used on a duplicate slide in place of the primary antibody as a negative control. Primary antibody was removed by PBST wash followed by incubation with goat anti-rabbit biotinylated secondary antibody and ABC reagent (Vector Universal kit; Vector Laboratories, Inc.) for 30 min each with interspersed PBST washes. The chromogen diaminobenzidine was applied for 5 min, and slides were counterstained with hematoxylin. Primary antibodies used include anti-activated caspase 3 (used at a 1:400 dilution; Cell Signaling) and anti-serine 10 phosphorylated histone H3 (used at a 1:1,500 dilution; Upstate).

Some slides were stained by immunofluorescence rather than immunocytochemistry. Sections were deparaffinized, rehydrated, and heated in 10 mM citric acid-PBST buffer for 20 min to retrieve antigenicity. Slides were blocked with 5% serum (matched to the species of the secondary antibody) in PBST for 1 h at room temperature and then incubated with primary antibody overnight at 4°C. Primary antibodies used were anti-Thoc1 (used at 1:1,000 dilution; Genetex), anti-GATA1 (used at 1:200 dilution; Santa Cruz Biotechnology), and antibodies TRA98 and TRA369 (both gifts of H. Tanaka and Y. Nishimune, Osaka University). Secondary antibodies used were goat anti-rabbit Alexa Fluor 488, donkey anti-goat Alexa Fluor 594, goat anti-mouse Alexa Fluor 488, goat anti-rabbit Alexa Fluor 594, and goat anti-rat Alexa Fluor 594 (Molecular Probes), all used according to the manufacturer's instructions.

Analysis of meiosis. Chromosome spreads were prepared from testes of P35 males as described previously (29). After washing with phosphate-buffered saline three times for 5 min, slides were processed for immunofluorescent staining as described above. Primary antibodies used include anti-RAD51 (used at 1:100 dilution; SC-8349; Santa Cruz Biotechnology), mouse anti-MLH1 (used at 1:100 dilution; Pharmingen), anti-phosphorylated histone H2AX (used at 1:500 dilution; Upstate Biotechnology), CREST antibody, and rabbit anti-SCP3 antibody (8). Red Alexa Fluor 560 and green Alexa Fluor 488-conjugated secondary antibodies were used according to manufacturer's recommendations (Molecular Probes).

Gene expression analysis. Total RNA from testis tissue was prepared using the RNeasy method according to manufacturer's recommendations (Qiagen, Inc.). RNA samples were concentrated by ethyl alcohol precipitation and resuspended in nuclease-free water. RNA concentration was quantitated using an ND-1000 spectrophotometer (NanoDrop) and evaluated for degradation using a 2100 Bioanalyzer (Agilent Technologies). For array analysis, only samples with an optical density at 260 nm (OD_{260})-to-OD_{280} ratio of 1.9 to 2.0 and a ratio of 28S:18S rRNA greater than 1.5 were used.

The cRNA probes for array analysis were synthesized and directly labeled with cyanine 3-CTP or cyanine 5-CTP using Agilent's low RNA input linear amplification method, per manufacturer's instructions (Agilent Technologies). First-strand cDNA was synthesized by incubating 0.2 to 2 μg total sample RNA, spike in controls, and oligo(dT) for 10 min at 65°C. Following the addition of first-strand reaction components, the reaction continued for 2 h at 40°C. The cRNA was synthesized by incubating the double-stranded cDNA with the transcription master mix containing cyanine-CTP, ribonucleotides, and T7 RNA polymerase for 2 h at 40°C. The cyanine-labeled cRNA was recovered by column purification and elution in RNase-free water. The cRNA quality and concentration were assessed using a NanoDrop ND-1000 UV-visible light spectrophotometer. cRNA samples were required to yield at least 750 ng with a specific activity of >8.0 pmol Cy3 or Cy5 per microgram cRNA for further use.

The labeled cRNA probes were hybridized to the 44K whole mouse genome oligo microarray (Agilent Technologies). Prior to hybridization, 0.75 μg of cyanine 5-labeled, linearly amplified cRNA (test) and 0.75 μg of cyanine 3-labeled, linearly amplified cRNA (control) were combined and fragmented by incubating at 60°C for 30 min in fragmentation buffer. The hybridization reaction mixture was placed on ice and then loaded onto the 44K array. The arrays were secured in a SureHyb chamber cover and hybridized at 65°C for 17 h. After hybridization, the slides were washed with gene expression wash buffers 1 and 2 (Agilent Technologies). Array images were captured by scanning at 532 nm and 635 nm with an Agilent scanner and analyzed with Agilent Feature Extraction software version 8.5. Feature Extraction files were first normalized within each array. Statistically significant differentially expressed genes were identified using the limma package from Bioconductor. The adjusted *P* values were calculated using the false discovery rate method.

Quantitative reverse transcription-PCR (RT-PCR). Real-time PCR using total testis RNA samples was performed using the ABI SYBR green method

(Applied Biosystems, Foster City, CA). Briefly, 50 ng RNA was mixed with SYBR green PCR master mix in the presence of primers. The PCR product was detected with the 7900HT fast real-time PCR system, and data were analyzed with ABI RQ Manager software. Primers used were as follows: *CDKN1A*, 5′-CCAGGCCAAGATGGTGTCTT-3′ and 5′-TGAGAAAGGATCAGCCATTGC-3′; *CCND2*, 5′-GGCCAAGATCACCCACACT-3′ and 5′-ATGCTGCTCTTGACGGAACT-3′; *GATA1*, 5′-TCACAAGATGAATGGTCAGA-3′ and 5′-TGGTCGTTTGACAGTTAGTG-3′; *CLU*, 5′-GGATTCTGAAATGAAGCTGAAGGC-3′ and 5′-TTCATGCAGGTATGCTTCAGGC-3′; *SOX9*, 5′-CGGAGGAAGTCGGTGAAGA-3′ and 5′-GTCGGTTTTGGGAGTGGTG-3′; *KIT*: 5′-GATCTGCTCTGCGTCCTGTT-3′ and 5′-CTGATTGTGCTGGATGGATG-3′; *RHOX5*, 5′-TCATCATTGATCCTATTCAGGGTATG-3′ and 5′-CTCTCCAGCCTGGAAGAAAGC-3′; *CDKN1C*, 5′-CACTCTGTACCATGTGCAAGGAGTA-3′ and 5′-TTTCTCTTTTTGTTTTGCACTGAGA-3′; *THOC1*, 5′-CATTCTATTCTGCTGGCAAAAATTAT-3′ and 5′-AAAGAGTTGAATTCTTCCACAGAAAAC-3′; *RB1*, 5′-CTTGAACCTGCTTGTCCTCTCA-3′ and 5′-GGAAGTTCTTTTCTTTGGAGATCTTAGA-3′; *GAPDH*, 5′-ACCCAGAAGACTGTGGATGG-3′ and 5′-CACATTGGGGGTAGGAACAC-3′.

ChIP. Chromatin immunoprecipitation (ChIP) analysis was performed using the ChIP assay kit with minor modifications of manufacturer's protocol (Upstate Biotechnology, Lake Placid, NY). Briefly, testes of 8-day-old mice were dissected, weighted, decapsulated, and fixed with 1% formaldehyde at room temperature for 15 min. Glycine was added to a final concentration of 125 mM for 5 min at room temperature. Testis tissue (0.02 g) was washed twice with phosphate-buffered saline and extracted with sodium dodecyl sulfate lysis buffer. Lysates were frozen at −80°C until use. Samples were sonicated at 4°C 30 times with a 10-s pulse followed by a 20-s gap. Supernatants were recovered by centrifugation at 13,400 × *g* (in an Eppendorf microcentrifuge) for 10 min at 4°C. Supernatants were diluted in ChIP dilution buffer and then precleared for 1 h at 4°C with 60 μl of salmon sperm DNA/protein A Sepharose (50% slurry). Immunoprecipitations were performed overnight with 1 μg of mouse anti-RNA POLII (Millipore Corporation), mouse anti-GAL4 (Calbiochem), or anti-THOC1 antibody (Genetex). The immune complexes were captured by incubation with 60 μl of protein A-Sepharose (50% slurry) for 1 h at 4°C. The beads were washed sequentially for 5 min each at 4°C in low-salt buffer, high-salt buffer, and LiCl buffer. Beads were washed twice with TE buffer (10 mM Tris-HCl, 1 mM EDTA [pH 8.0]) and eluted with 30 μl of elution buffer (1% sodium dodecyl sulfate, 0.1 M $NaHCO_3$).

To reverse the cross-links, samples were incubated in 200 mM NaCl at 65°C overnight. Supernatants were then incubated for 30 min at 37°C with RNase A and 1 h at 45°C with proteinase K, in 40 mM Tris-HCl (pH 6.5) and 10 mM EDTA. DNA was recovered by phenol-chloroform extraction followed by ethanol precipitation in the presence of 20 μg glycogen. The DNA pellet was washed with 70% ethanol, air dried, and resuspended in 30 μl water and for use as a template for PCR.

Primers used for ChIP assay were as follows: *RHOX5*, 5′-TCGCCATACTTTGGAGAGAGA-3′ and 5′-CCTGCTAAACATTCCTGACCA-3′; 5′ *GATA1*, 5′-CAACAAGCCCAGGTCAGTCT-3′ and 5′-CCGTTTTAGGGGCAACCTAT-3′; Middle *GATA1*, 5′-GCACTCTACCCTGCCTCAAC-3′ and 5′-GCTCTTCCCTTCCTGGTCTT-3′; 3′ *GATA1*, 5′-GCTCCAGCTTGAGATCCTTG-3′ and 5′-GGAGATGGTTGGGCTGTAAA-3′; *KIT*, 5′-GGCGAGAGCTGTAGCAGAGA-3′ and 5′-CAACAGGACGCAGAGCAGAT-3′; *PPT1*, 5′-GATTGCTAAGATGGCGTCGT-3′ and 5′-GGTGAAGGTGGGTCCAGAT-3′; *AMHRII*, 5′-GTGCTGGTTTTTGCTGGTTT-3′ and 5′-GCCCCGCTCTGTAGACTCTT-3′; *VDR*, 5′-AGCCCTAAGCACGGGAAG-3′ and 5′-CCGGGTCTAACCACTCACC-3′; *VIM*, 5′-CCAGGGATCGCTTTACTCAA-3′ and 5′-TTGGGTGCTGAGAAAGAAGG-3′; *IMPDH2*, 5′-CTGTCTTCCTCCGTGGTCAT-3′ and 5′-CCCTAGACCCGCACTTGTAG-3′.

RESULTS

***Thoc1* deficiency compromises male and female fertility.** We attempted to breed male mice containing hypomorphic alleles of *Thoc1* with wild-type females. $Thoc1^{H/+}$ male mice sired offspring normally and did not exhibit any phenotypes distinguishable from the wild type. As such, both wild-type and $Thoc1^{H/+}$ males were used equivalently as littermate controls for the remainder of the study. None of the 10 $Thoc1^{H/H}$ male mice tested were able to sire offspring (Table 1). The mating behavior of $Thoc1^{H/H}$ male mice appeared normal as indicated by the presence of the postcopulatory vaginal plug. We also attempted to breed five of $Thoc1^{H/H}$ male mice with superovulated wild-type females, but no offspring were sired despite the presence of vaginal plugs in four out of five females. Embryos were retrieved from wild-type females mated with $Thoc1^{H/H}$ or littermate control mice 1 day following detection of the vaginal plug. Only unfertilized or degenerating oocytes were recovered from females mated with $Thoc1^{H/H}$ males (Fig. 1A). Normal two-cell stage embryos were obtained from females mated with littermate control mice. Consistent with these observations, total sperm counts and the percentage of motile sperm were significantly reduced in $Thoc1^{H/H}$ males compared to those in wild-type males (Fig. 1B and C).

TABLE 1. Fertility of hypomorphic *Thoc1* mice

Genotype[a]	No. of males	No. of females	No. (%) of pregnant mice	Mean no. of pups/litter
+/+ × +/+	2	4	4 (100)	5.5 ± 1.9
H/+ × +/+	8	8	8 (100)	6.4 ± 2.1
H/*H* × +/+	10	14	0 (0)[b]	0
+/+ × *H*/+	9	9	9 (100)	6.4 ± 1.9
+/+ × *H*/*H*	15	36	5 (14)[b]	1.6 ± 0.6[c]

[a] Genotypes are male × female, with *H* designating the hypomorphic allele.
[b] Significantly different from wild-type mating, based on Fisher's exact test ($P \leq 0.05$).
[c] Significantly different from wild-type mating, based on Student's *t* test ($P \leq 0.05$).

We also mated $Thoc1^{H/H}$ female mice with wild-type males. Vaginal plugs were observed in all $Thoc1^{H/H}$ females tested. From a total of 23 female $Thoc1^{H/H}$ mice, one gave birth to a single live pup that subsequently matured with no obvious phenotype distinguishable from the wild type. Four other $Thoc1^{H/H}$ females became pregnant, but their pups were found dead shortly after birth. The litter size from these five $Thoc1^{H/H}$ females was significantly smaller than normal (Table 1). Furthermore, each of these females became pregnant only once despite subsequent attempts at mating. Thus, the fertility of both male and female $Thoc1^{H/H}$ mice was severely compromised compared to that of wild-type mice.

Abnormal testis development in $Thoc1^{H/H}$ mice. $Thoc1^{H/H}$ mice were smaller than their wild-type littermates (37). However, organ weights of $Thoc1^{H/H}$ mice were proportional to body weight (Fig. 2A). In conjunction with the observation that most $Thoc1^{H/H}$ mice live a normal life span, it appears that the development and function of most tissues were relatively normal despite *Thoc1* deficiency. The one exception noted was the testes, where the relative organ weight was significantly less than that in littermate control mice. Since hypogonadism and infertility have been associated with disrupted endocrine signaling and feedback control, we measured the serum levels for a number of different hormones. Levels of growth hormone and insulin-like growth factor 1 in $Thoc1^{H/H}$ mice were not significantly different than those in control mice (see Fig. S1A and B in the supplemental material). Serum testosterone and luteinizing hormone (LH) levels varied considerably from mouse to mouse, but both were typically higher in $Thoc1^{H/H}$ mice than in control mice (see Fig. S1C and D in the supplemental material). Male transgenic mice engineered to express serum levels of LH/human chorionic gonadotrophin (hCG) comparable to those expressed by $Thoc1^{H/H}$ mice, a three- to

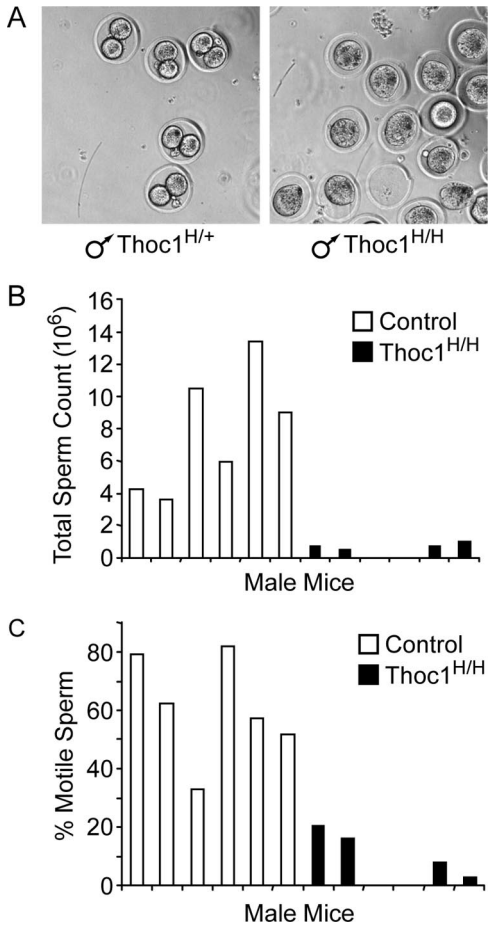

FIG. 1. *Thoc1*$^{H/H}$ mice are infertile due to lack of viable sperm. (A) Representative phase contrast photomicrograph (×50 magnification) of E1.5 embryos produced by mating the indicated male mice with wild-type females. (B) Sperm in the cauda epididymis of individual mice of the indicated genotype were counted using a hemacytometer. Two of the five *Thoc1*$^{H/H}$ mice contained no detectable sperm. (C) The percentage of sperm with an active flagellum is shown. Each bar represents an individual mouse of the indicated genotype.

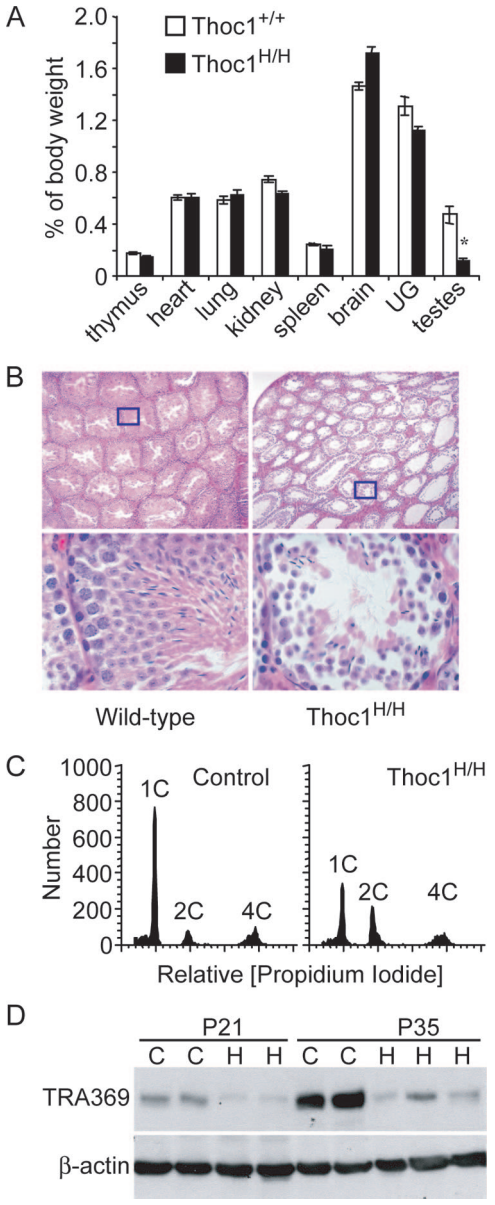

FIG. 2. Loss of spermatocytes and spermatids in adult *Thoc1*$^{H/H}$ testes. (A) Four-month-old mice were dissected, and the wet weight of individual organs, relative to total body weight, were measured and expressed. The data show the mean and standard deviation from five mice for each of the indicated genotypes. The asterisk indicates a significant deviation from the wild-type control based on Student's *t* test ($P < 0.01$). UG, urogenital tract. (B) Testes from adult mice of the indicated genotypes were dissected and processed for sectioning. The upper panels are representative hematoxylin- and eosin-stained bright-field photomicrographs (×40 magnification) showing a field of seminiferous tubules. The boxes indicate a region magnified ×400 in the lower panel images. (C) Single cell suspensions from testes of 3-month-old mice of the indicated genotypes were stained with propidium iodide and analyzed by flow cytometry. A representative histogram is shown. Three major populations of cells are resolved based on their relative DNA contents. The 1C peak and shoulder include round and elongating spermatids. The 2C peak primarily includes somatic cells and spermatogonia. The 4C peak is composed primarily of spermatocytes. (D) Protein extracts were prepared from testes from mice of the indicated genotypes at P21 and P35. The protein extracts were analyzed by Western blotting using the TRA369 antibody that recognizes an antigen expressed in the pachytene spermatocyte through elongated spermatid stages of spermatogenesis. The blot was also probed with an antibody specific for β-actin to serve as a loading control.

fourfold increase relative to those expressed by wild-type mice, are fertile and display only a mild phenotype (31). Thus, while disruption of normal endocrine signaling likely contributes to the observed phenotype, the changes in serum hormone levels observed are unlikely to completely account for the sterility of *Thoc1*$^{H/H}$ male mice.

To investigate whether defects in testis development contribute to the sterility of *Thoc1*$^{H/H}$ mice, we examined the histology of *Thoc1*$^{H/H}$ testes. Consistent with the data shown in Fig. 1, very few spermatocytes, spermatids, or mature spermatozoa were observed in adult *Thoc1*$^{H/H}$ mice (Fig. 2B). The number of cells with 1C DNA content (spermatids) relative to the number cells with 2C DNA content (primarily somatic cells and premeiotic germ cells) was lower in *Thoc1*$^{H/H}$ testes (2.3 ± 0.9; $n = 3$) than in control testes (4.4 ± 0.6; $n = 3$) as quantitated by flow cytometry (Fig. 2C). The relative number of cells with 4C DNA content (primary spermatocytes and G_2 phase somatic cells) was also significantly lower in *Thoc1*$^{H/H}$ testes (0.9 ± 0.27) than in control testes (1.6 ± 0.02). Loss of

spermatocytes and spermatids was confirmed by Western blot analysis of testis protein extracts using antibody TRA369. TRA369 recognized an antigen expressed specifically by germ cells at the pachytene spermatocyte through elongated spermatid stages (15, 26). A significant decrease in expression of this antigen was apparent at postnatal day 21 (P21) in *Thoc1*$^{H/H}$ testes compared to that in control testes (Fig. 2D). It should be noted that some normal-appearing spermatids and spermatozoa were observed in *Thoc1*$^{H/H}$ mice. Thus, we could not rule out the possibility that some functional sperms do arise in these mice but presumably in numbers insufficient to support fertility.

We have examined testes in younger mice to determine when defects in the *Thoc1*$^{H/H}$ testes can first be detected. At P1, developing seminiferous tubules are composed of somatic Sertoli cells at the periphery and centrally located prospermatogonia. At this age, the histology of *Thoc1*$^{H/H}$ testes is indistinguishable from that of control testes (Fig. 3A). Expression of nuclear pThoc1 is apparent in Sertoli cells of wild-type testes, but not obviously in prospermatogonia. Nuclear pThoc1 is not readily detectable in *Thoc1*$^{H/H}$ testes. Cytoplasmic staining is also observed in these sections, but at least some of this is background. By P6, prospermatogonia migrate to a basal position within the tubule and differentiate into type A spermatogonia. The first wave of meiosis begins around P8. At P8, *Thoc1*$^{H/H}$ tubules are slightly smaller in diameter than those in control mice, and they lack an obvious lumen. As in P1 *Thoc1*$^{H/H}$ testes, little nuclear pThoc1 staining is observed. Wild-type testis tubules are developing an obvious lumen. Thoc1 protein is present in the nuclei of Sertoli cells, and punctate nuclear staining is observed in germ cells at certain developmental stages. By P14, the difference in size between *Thoc1*$^{H/H}$ and control testes is more pronounced, and *Thoc1*$^{H/H}$ testis tubules still lack an obvious lumen. By P21, lumens have become apparent in *Thoc1*$^{H/H}$ testis tubules (data not shown), suggesting that there is a delay in the migration of prospermatogonia to a basal position within the tubule.

To verify this, we stained testis sections using the stage-specific antibody TRA98. TRA98 recognizes an antigen expressed in prospermatogonia and spermatogonia, but not in cells at later stages of spermatogenesis (15, 26). TRA98-positive cells are present in P1 *Thoc1*$^{H/H}$ and control testes in similar numbers. By P8, control TRA98-positive germ cells have migrated from a central to a basal position within the tubule. Most *Thoc1*$^{H/H}$ TRA98-positive cells have failed to migrate by P14 (Fig. 3C). This observation confirms that *Thoc1*$^{H/H}$ germ cells fail to migrate normally prior to the first wave of meiosis.

Seminiferous tubules have a decreased diameter in *Thoc1*$^{H/H}$ testes compared to that in control testes. The decrease in tubule size is not likely due to reduced cell proliferation during postnatal development, as the percentage of Ki67 or phosphorylated histone H3-positive cells in *Thoc1*$^{H/H}$ tubules is actually higher than that in controls (see Fig. S2 in the supplemental material). Since testes from P21 and older *Thoc1*$^{H/H}$ mice contain very few spermatocytes, it is possible that the spermatocytes are dying during the first wave of meiosis. To examine this possibility, we have assessed the percentage of apoptotic cells in testis sections by immunostaining the activated form of caspase 3. At P1, activated caspase 3-positive

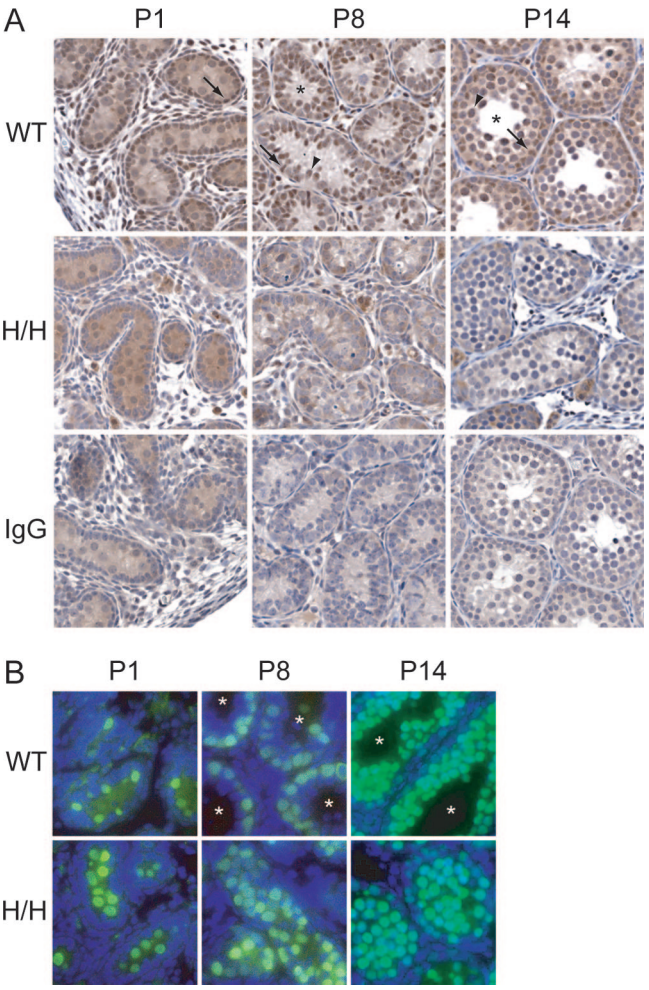

FIG. 3. Histology of seminiferous tubules during postnatal development. (A) Testes from wild-type and *Thoc1*$^{H/H}$ mice at the indicated postnatal days of development were fixed, sectioned, and immunostained with a polyclonal antibody specific for pThoc1. The bottom panels show testis sections from wild-type mice stained with a preimmune control antibody. Representative photomicrographs showing a 200-μm square field is shown. The asterisks indicate the developing lumen of the seminiferous tubule that forms as early as P8 in wild-type mice. The arrows indicate representative Sertoli cells showing nuclear pThoc1 staining. The arrowheads show representative germ cells with stage-specific, punctate nuclear pThoc1 staining. (B) Testis sections from wild-type and *Thoc1*$^{H/H}$ mice at the indicated postnatal days of development were stained with TRA98 antibody that recognizes spermatogonia (green). Cells were counterstained with Hoechst 33342 (blue). The asterisks highlight the tubule lumen and the migration of spermatogonia to a basal position by P8 in wild-type mice.

cells are rarely observed in either *Thoc1*$^{H/H}$ or control testes (data not shown). By P8, the percentage of testis tubules containing activated caspase 3-positive cells is significantly higher in *Thoc1*$^{H/H}$ mice than that in control mice (Fig. 4A). The fraction of apoptotic cells peaks at P14 and subsequently declines by P21. Similar results are obtained using the terminal deoxynucleotidyltransferase-mediated dUTP-biotin nick end labeling assay to stain cells with fragmented DNA (see Fig. S3 in the supplemental material). To assess whether the dying cells are spermatocytes, we have analyzed the distribution of testes cells with 4C (primary spermatocytes) and 2C (sper-

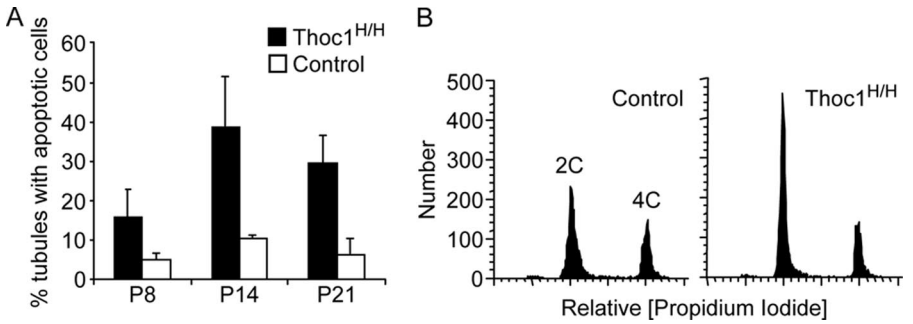

FIG. 4. Loss of spermatocytes due to apoptotic cell death in *Thoc1*$^{H/H}$ mice. (A) Testis sections from control and *Thoc1*$^{H/H}$ mice of the indicated postnatal days of development were immunostained with antibody specific for the activated form of caspase 3 to mark apoptotic cells. The percentage of seminiferous tubules containing apoptotic cells from an average of 200 total tubules counted per sample was determined. The data show the mean and standard deviation for at least three mice per data point. Data from *Thoc1*$^{H/H}$ mice are significantly different from those from control mice at each time point (Student's *t* test; $P < 0.05$). (B) Single-cell suspensions from P14 testes of the indicated genotypes were stained with propidium iodide and analyzed by flow cytometry. A representative histogram is shown. Two major populations of cells are resolved based on their relative DNA content. The 2C peak primarily includes somatic cells and spermatogonia. The 4C peak is composed primarily of spermatocytes.

matogonia and somatic cells) DNA content at P14 by flow cytometry. The number of 4C cells relative to the number of 2C cells is significantly reduced in *Thoc1*$^{H/H}$ testes compared to in control testes (Fig. 4B). Thus, the increased apoptosis detected in *Thoc1*$^{H/H}$ testes correlates with a loss in the relative number of primary spermatocytes.

We note that there is variation in the severity of the testis phenotype in *Thoc1*$^{H/H}$ mice. While all male *Thoc1*$^{H/H}$ mice are sterile, some mice have a near complete lack of sperm, while others have a low but significant number (Fig. 1B; also see Fig. S4A in the supplemental material). Comparing testis pThoc1 expression in mice with mild and severe phenotypes, we observe higher levels of pThoc1 in mice with a milder phenotype (see Fig. S4B in the supplemental material). Thus, the severity of the testis phenotype is inversely correlated with pThoc1 levels.

***Thoc1* is not required for synaptonemal complex formation or progression through meiotic prophase.** It is not obvious why gametogenesis is particularly sensitive to *Thoc1* deficiency. Loss of *Thoc1* in yeast causes a hyperrecombination phenotype due to the formation of RNA:DNA hybrids at sites of stalled transcription complexes (38). It is conceivable that a related defect in *Thoc1*$^{H/H}$ mice may compromise normal DNA recombination that occurs during meiosis and, thus, adversely affecting spermatocyte viability.

To test this, we have analyzed chromosome structure during meiotic prophase by immunofluorescent staining of spermatocytes from 5-week-old mice. Anti-COR1/SCP3 antibody recognizes a component of the lateral element of the synaptonemal complex, while CREST antibody can be used to stain centromeres (8). MLH1 protein is present in foci at sites of DNA recombination during meiosis (20, 24). Although fewer spermatocytes are retrieved from *Thoc1*$^{H/H}$ mice, the staining of centromeres, synaptonemal complexes, and MLH1 is similar to that observed in spermatocytes from control mice (Fig. 5A). The numbers of MLH1 foci per spermatocyte are also similar in *Thoc1*$^{H/H}$ and control mice (Fig. 5B). The staining of γ-H2AX also appears normal in *Thoc1*$^{H/H}$ spermatocytes (data not shown). These observations indicate that synaptonemal complex formation and meiotic recombination are not detectably altered in *Thoc1*-deficient mice.

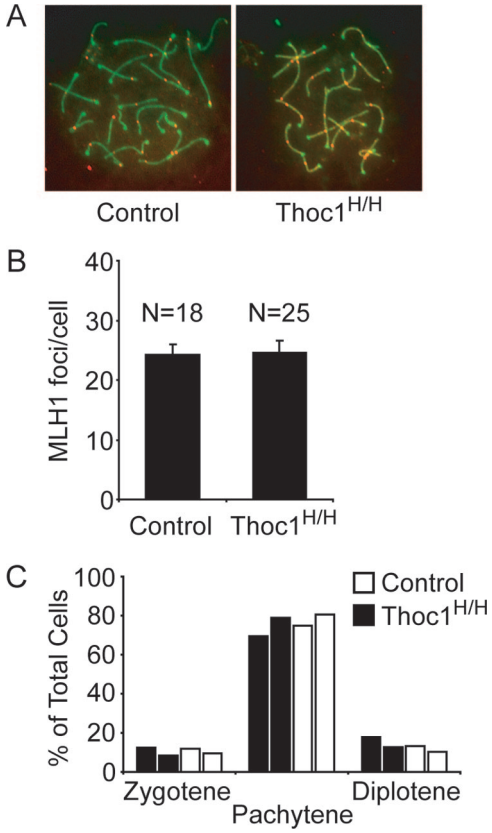

FIG. 5. Meiosis appears normal in spermatocytes from *Thoc1*$^{H/H}$ mice. (A) Spermatocyte chromosome spreads were prepared from P35 mice of the indicated genotypes and immunostained to identify the synaptonemal complex and centromeres (SCP3, CREST [green]) and chiasmata (MLH1 [red]). Representative photomicrographs captured under fluorescent microscopy at ×400 magnification are shown. (B) MLH1 foci, which represent sites of meiotic DNA recombination, were counted on spermatocyte chromosome spreads stained as described above. The data are expressed as the mean number of MLH1 foci per spermatocyte ± standard deviation for the indicated sample size (N). (C) Chromosome spreads from control and *Thoc1*$^{H/H}$ mice were prepared and immunostained for CREST, SCP3, and H1t. More than 100 prophase spermatocytes for each mouse were scored for their stage in meiosis. The figure shows the relative percentage of spermatocytes at the indicated stages of meiosis. Each bar series represents results from a single mouse.

To assess the progression of spermatocytes through the pachytene stage, where chromosome crossing-over occurs, we counted the relative numbers of zygotene (before recombination), pachytene (during recombination), and diplotene (after recombination) cells, using chromosome morphology and stage-specific markers. We found that the relative distributions of zygotene, pachytene, and diplotene spermatocytes are similar in *Thoc1*$^{H/H}$ and control mice (Fig. 5C). Thus, the progression of spermatocytes through meiotic prophase is not detectably affected by *Thoc1* deficiency.

***Thoc1* is required for normal gene expression during postnatal testis development.** A second potential mechanism underlying sterility is that *Thoc1* deficiency compromises the expression of genes necessary for normal testis development. To assess this possibility, we performed gene expression profiling of P8 testes from *Thoc1*$^{H/H}$ and control mice. We chose to analyze P8 mice, as a phenotype is first detected in *Thoc1*$^{H/H}$ testes at this age (prospermatogonia migration defect). Furthermore, spermatocyte apoptosis is infrequent in *Thoc1*$^{H/H}$ testes at this age, so gene expression profiling will not be biased by changes in the composition of the tissue. Using a twofold difference in signal between *Thoc1*$^{H/H}$ and control samples as the cutoff value, we found that the expression of about 3% of genes was altered by *Thoc1* deficiency. About half of the affected genes were downregulated in *Thoc1*$^{H/H}$ testes relative to those in control testes. As expected, *Thoc1* was one of these downregulated genes, as it showed a fivefold decrease in signal. Downregulation of pThoc1 levels was confirmed by Western blotting of wild-type and *Thoc1*$^{H/H}$ testis extracts (see Fig. S4B in the supplemental material).

Mouse testes at P8 are primarily comprised of three cell types. The germ and Sertoli cells are the major cell types within the developing seminiferous tubules, while Leydig cells are the main interstitial cell type. We have examined in greater detail a number of genes that have a demonstrated role in these cell types and/or whose expression is enriched in these cell types. Twenty-six out of 52 of these genes show a significant change in expression in *Thoc1*$^{H/H}$ testes (adjusted *P* value of $\leq$0.05). Of these 26, 5 are upregulated, and 21 are downregulated (see Table S1 in the supplemental material). We verified the microarray data by quantitative RT-PCR and immunofluorescent staining. RT-PCR data confirmed the altered expression of several genes in *Thoc1*$^{H/H}$ testes and more generally demonstrated good correlation with the microarray data (Fig. 6A). Decreased expression of *GATA1* protein, one of the gene products affected by *Thoc1* deficiency, was verified by immunostaining of testis tissue sections (Fig. 6B). The greatest change observed in *Thoc1*$^{H/H}$ testes is a decrease in the expression of *RHOX5*. *RHOX5* is a homeobox transcription factor that in postnatal mice is expressed primarily in the testes (Sertoli cells), epididymis (principal cells of the caput region), and ovaries (preovulatory follicles) (33). *RHOX5* is required for spermatogenesis, as deletion of *RHOX5* leads to reduced fertility, increased germ cell apoptosis, lower sperm counts, and reduced sperm motility (19).

Most of the genes whose expression was altered by *Thoc1* deficiency, like *RHOX5*, show a decrease in expression. Many of these affected genes are expressed in Sertoli cells, a cell type where pThoc1 is also expressed. This suggests the possibility that a number of these genes may be direct targets for regulation by pThoc1. To explore this possibility further, we have analyzed wild-type testis extracts by ChIP. ChIP with pThoc1 or POLII antibodies capture readily detectable promoter-proximal DNA from the *GATA1*, *RHOX5*, *VDR*, and *AMHR2* genes (Fig. 7A). Although *KIT* expression declines in *Thoc1*$^{H/H}$ testes, the signal from pThoc1 ChIP of *KIT* is relatively low compared to that from POLII ChIP. Similarly, the pThoc1 ChIP signal from two genes whose expression is unaffected by pThoc1 deficiency, *IMPDH2* and *VIM*, is also relatively low. Low pThoc1 occupancy of *KIT*, *IMPDH2*, and *VIM* suggests that they may not be directly regulated by pThoc1. However, we cannot rule out the possibility that they are directly regulated by pThoc1 in only a fraction of the cells assayed, that pThoc1 occupies regions of these genes not interrogated by PCR, or that the relatively low signal is due to limitations in semiquantitative PCR.

Thoc1 deficiency has been associated with a transcriptional elongation defect in both yeast and mammalian cells (5, 18, 30). If genes are direct targets for pThoc1 regulation, then POLII occupancy should decrease in *Thoc1*$^{H/H}$ testes, particularly toward the 3′ end of the gene due to a transcriptional elongation defect. ChIP analysis of *RHOX5*, *AMHR2*, *GATA1*, and *KIT* has been repeated with *Thoc1*$^{H/H}$ testis extracts, and the results were compared to those with wild-type extracts.

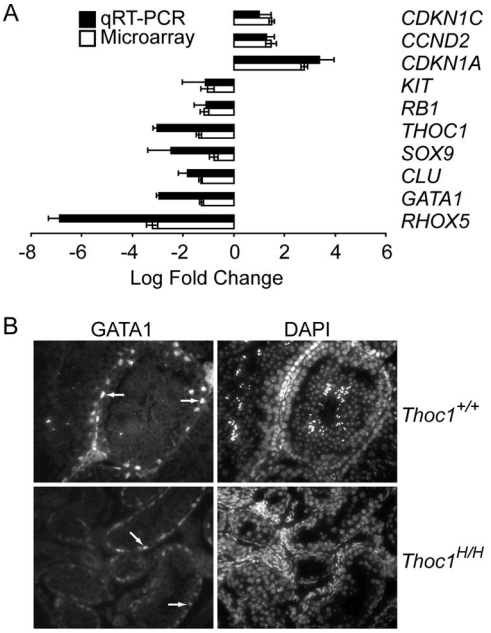

FIG. 6. Gene expression changes in *Thoc1*$^{H/H}$ testes. (A) Testes from P8 mice were isolated, RNA was extracted, and gene expression was examined by microarray or quantitative PCR analysis. The data show the mean log base 2 change ± standard deviation of the signal from *Thoc1*$^{H/H}$ mice compared to that for control mice for each method. RNA from four individual *Thoc1*$^{H/H}$ mice was compared to a reference pool composed of four littermate control mice. All of the gene expression changes displayed are significant, based on an adjusted *P* value of <0.05. (B) Testes sections from P35 wild-type and *Thoc1*$^{H/H}$ mice were immunostained for *GATA1* protein (left panels) and counterstained with DAPI (4′,6-diaminidino-2-phenylindole) (right panels). Representative photomicrographs captured under fluorescence microscopy at ×100 magnification are shown. Arrows indicate intense staining of Sertoli cells in wild-type testes and reduced staining of Sertoli cells in *Thoc1*$^{H/H}$ testes.

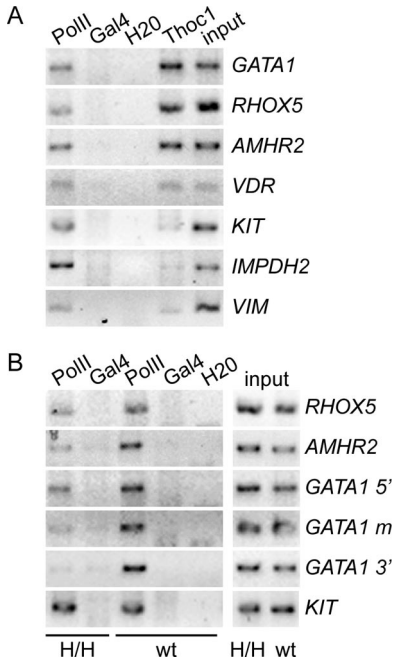

FIG. 7. Some genes affected in *Thoc1*$^{H/H}$ mice are direct targets for regulation by pThoc1. (A) Testes from four P8 wild-type mice were pooled and analyzed by ChIP. Chromatin immunoprecipitated with a pThoc1 antibody was compared to chromatin immunoprecipitated with POLII (positive control) or GAL4 (negative control) antibodies. The input lane represents 2% of the extract used for immunoprecipitation. The H2O lane contains no DNA template. Promoter proximal primers for the indicated genes were used to amplify the DNA, PCR fragments were resolved by agarose gel electrophoresis, and the fragments were stained by ethidium bromide. The signals on the representative gel images shown were inverted for clarity. (B) Testes from four P8 *Thoc1*$^{H/H}$ mice were pooled and compared with the wild-type sample for POLII occupancy at the indicated genes as described above. The promoter-proximal PCR primers used for each gene were as described above, except that additional primers mapping to the middle (m) and 3′ end of the *GATA1* gene were also used. The input for each sample was normalized for each primer pair and was verified to be within the linear range of the PCR assay (see Fig. S5 in the supplemental material).

POLII ChIP captures less promoter-proximal DNA from *Thoc1*$^{H/H}$ testis extracts than from wild-type extracts for each gene examined, except *KIT*. POLII ChIP captures equal levels of *KIT* DNA from both extracts, again suggesting that *KIT* is not directly affected by pThoc1 deficiency. ChIP analysis of *GATA1* has been extended to include PCR primers for the middle and 3′ end of the gene. In *Thoc1*$^{H/H}$ testis extracts, but not in wild-type extracts, POLII ChIP captures progressively less *GATA1* DNA moving toward the 3′ end of the gene (Fig. 7B). This observation indicates that POLII occupancy declines toward the 3′ end of the gene in pThoc1-deficient cells, consistent with a transcriptional elongation defect at *GATA1*. To ensure that the ChIP analysis was semiquantitative, we normalized input DNA for each extract within the linear range of the PCR assay (see Fig. S5 in the supplemental material). In sum, the ChIP analysis is consistent with the hypothesis that some, but not all, genes affected in *Thoc1*$^{H/H}$ testes are direct targets for regulation by pThoc1.

DISCUSSION

We have used a hypomorphic *Thoc1* allele to study the effects of pThoc1 deficiency on postnatal development and cellular differentiation in the mouse. Given the early embryonic lethality associated with *Thoc1* nullizygosity and its widespread expression in embryonic and postnatal tissue (36), it is surprising that hypomorphic *Thoc1* mice are viable. While these hypomorphic mice are smaller than their wild-type littermates (37), they appear otherwise normal, and most live a typical life span. Given the viability of the hypomorphic mice, it appears that many tissues can tolerate significantly reduced levels of pThoc1.

The exceptions noted here are the testes and ovaries, as the fertility of both male and female hypomorphic *Thoc1* mice is severely diminished. Hypomorphic males never successfully sire offspring, despite evidence of normal mating behavior. Similarly, most hypomorphic females fail to conceive, although a few females do become pregnant. However, these females become pregnant only once, despite repeated attempts at mating. In males, infertility is associated with a reduction in the number of viable spermatocytes. While a few normal-appearing sperm are detectable in some hypomorphic mice, the percentage of these sperm with active flagellum is low compared to that of wild-type sperm. This suggests that even surviving spermatocytes suffer from additional defects during spermiogenesis. We cannot exclude the possibility that normal functioning sperm are produced in *Thoc1*$^{H/H}$ mice, but in numbers insufficient to support fertility.

We have considered a number of explanations to account for the tissue-restricted phenotype of *Thoc1*$^{H/H}$ mice. Expression of pThoc1 is widespread in both mouse embryos and adults (36), and pThoc1 levels are significantly reduced in other tissues of *Thoc1*$^{H/H}$ mice without obvious phenotypic effect. For example, the brain expresses relatively high levels of pThoc1, and pThoc1 levels are significantly reduced in *Thoc1*$^{H/H}$ brains (37). Yet, there is no gross anatomical brain phenotype or behavioral defects in hypomorphic mice. Thus, the expression pattern of *Thoc1* alone does not explain the observed tissue-restricted phenotype.

Normal testis development and function are reliant on interdependent interactions between the various cell types present, as well as systemic endocrine signaling. As pThoc1 deficiency is widespread in *Thoc1*$^{H/H}$ mice, it is likely that observed defects in endocrine signaling contribute to the observed testis phenotype. However, we argue that observed changes in serum hormone levels cannot completely account for the sterility of *Thoc1*$^{H/H}$ mice. It is true that transgenic mice engineered to express high levels of LH/hCG are sterile (32). However, these LH/hCG-overexpressing mice achieve serum LH/hCG levels up to 2,000-fold higher than those achieved by wild-type mice and exhibit enlarged seminal vesicles and prostates. *Thoc1*$^{H/H}$ mice, on the other hand, only exhibit a three- to fourfold increase in serum LH levels compared to those exhibited by control mice and do not show an increased mass of urogenital tissues (Fig. 2A). Indeed, transgenic mice engineered to overexpress more-modest levels of LH/hCG comparable to those observed in *Thoc1*$^{H/H}$ mice are fertile and exhibit very mild phenotypes (31). Given that pThoc1 is expressed in the testes during postnatal development and that

this expression is reduced considerably in mice homozygous for the hypomorphic allele, we conclude that cell autonomous defects make a significant contribution to the observed sterility of *Thoc1*$^{H/H}$ mice.

Based on a known molecular defect associated with *Thoc1* deficiency in yeast, we have explored whether reduced pThoc1 levels compromise meiosis. Loss of *Thoc1* in yeast is associated with a hyperrecombination phenotype caused when DNA replication complexes collide with stalled transcription complexes (38). A similar defect in pThoc1-deficient spermatocytes may conceivably interfere with normal meiotic DNA recombination. However, we have been unable to detect meiotic defects in spermatocytes from *Thoc1*$^{H/H}$ testes. Synaptonemal complex formation appears normal in *Thoc1*$^{H/H}$ spermatocytes. These spermatocytes also appear to transit normally through prophase, as indicated by a normal distribution of zygotene, pachytene, and diplotene stage cells. The extent of meiotic DNA recombination also appears normal, since the numbers of MLH1-positive foci observed along the meiotic chromosomes of *Thoc1*$^{H/H}$ and wild-type mice are similar. The staining patterns of γ-H2AX are also similar in wild-type and *Thoc1*$^{H/H}$ spermatocytes (data not shown). While we cannot exclude the presence of more-subtle meiotic defects, such defects appear unlikely to account for the initial testis phenotype observed *Thoc1*$^{H/H}$ mice.

The first testis phenotype detected in *Thoc1*$^{H/H}$ mice is the failure of prospermatogonia to migrate from the center of the developing seminiferous tubule to a basal position. Physical interaction between Sertoli cells and prospermatogonia is critical for this migration, for creation of the germ stem cell niche, and for subsequent spermatogenesis (34). Given the documented effects of pThoc1 on transcriptional elongation and gene expression, we have explored the possibility that pThoc1 regulates a gene expression program necessary for the normal differentiation of these cells within the developing testis. Of a subset of genes that have a documented role in testis development, or whose expression is restricted to the testes, 50% show altered expression in hypomorphic *Thoc1* mice. Of the genes showing altered expression, 84% are downregulated in *Thoc1*$^{H/H}$ testes, a figure significantly different from random. As pThoc1 deficiency is expected to reduce gene expression, this suggests that a number of these genes may be directly regulated by pThoc1.

ChIP data presented here are consistent with this possibility. For example, *GATA1* is normally expressed on mature Sertoli cells (34). *Thoc1* also appears to be expressed in Sertoli cells (Fig. 3). *GATA1* RNA and protein levels are significantly reduced in *Thoc1*$^{H/H}$ testes (Fig. 6). *Thoc1* protein is present at the *GATA1* gene. Importantly, POLII occupancy of *GATA1* progressively declines from the 5′ to the 3′ end of the gene in pThoc1-deficient testes, but not in wild-type testes (Fig. 7). This suggests the presence of a transcriptional elongation defect at *GATA1* in *Thoc1*-deficient cells, consistent with documented molecular defects associated with *Thoc1* deficiency in yeast and cultured mammalian cells. We note that pThoc1 does not occupy all genes whose expression is affected by *Thoc1* deficiency. Nor does it efficiently occupy genes whose expression is unaffected by pThoc1 deficiency. Thus, regulation by pThoc1 is likely restricted to a specific subset of genes. Approximately 3% of genes interrogated by our microarray are significantly altered in *Thoc1*$^{H/H}$ testes. Many of these gene expression changes, particularly those where expression is increased in *Thoc1*$^{H/H}$ mice, are most likely indirect consequences of *Thoc1* deficiency.

We conclude that pThoc1 directly regulates the expression of a number of genes required for functional differentiation of cells within the testes. In the absence of normal pThoc1 levels, expression of these genes is reduced, thereby causing defects in spermatogenesis and consequent infertility. For example, *RHOX5* is normally expressed in postnatal Sertoli cells and is required to maintain the viability of germ cells in the testes. *RHOX5* knockout mice display a phenotype reminiscent of that of hypomorphic *Thoc1* mice, including increased germ cell apoptosis, compromised sperm motility, and reduced fertility (19). Thus, the decrease in *RHOX5* expression in *Thoc1*$^{H/H}$ testis may contribute to the resulting phenotype, although other alterations in gene expression likely contribute, since the phenotype of *RHOX5* knockout mice is milder than that observed here. Defects in the functional maturation of Sertoli cells are also suggested by the decrease in expression of genes like *GATA1* that are normally expressed in mature Sertoli cells and by the increase in expression of genes like *KRT18* that are normally expressed in immature Sertoli cells (34). Sertoli cell dysfunction may account, in part, for the defect in prospermatogonia migration observed in early postnatal *Thoc1*$^{H/H}$ testes.

Thoc1 encodes a protein involved in RNP biogenesis and RNA processing. The data presented here demonstrate that a systemic deficiency of pThoc1 has specific and tissue-restricted effects on gene expression and tissue development. In particular, gene expression that supports the developing postnatal testis is compromised by pThoc1 deficiency. A number of the genes affected are likely direct targets for regulation by pThoc1. These observations support the hypothesis that RNP biogenesis is required for the coordinated expression of genes necessary for cellular differentiation in vivo.

ACKNOWLEDGMENTS

The paper is dedicated to the memory of our colleague Peter Moens.

We thank members of the Goodrich and Moens labs for helpful discussions and critical insight.

This work was supported by NCI grant CA125665 (to D.W.G.). NCI Cancer Center Support Grant CA016056 supported the Cell Analysis, Transgenic Mouse, and Gene Expression Core facilities used in this work. The Vanderbilt Hormone Assay & Analytical Services Core is supported in part by NIH grant U24 DK59637.

REFERENCES

1. **Abruzzi, K. C., S. Lacadie, and M. Rosbash.** 2004. Biochemical analysis of TREX complex recruitment to intronless and intron-containing yeast genes. EMBO J. **23:**2620–2631.
2. **Blake, W. J., M. Kaern, C. R. Cantor, and J. J. Collins.** 2003. Noise in eukaryotic gene expression. Nature **422:**633–637.
3. Reference deleted.
4. **Chang, M., D. French-Cornay, H. Y. Fan, H. Klein, C. L. Denis, and J. A. Jaehning.** 1999. A complex containing RNA polymerase II, Paf1p, Cdc73p, Hpr1p, and Ccr4p plays a role in protein kinase C signaling. Mol. Cell. Biol. **19:**1056–1067.
5. **Chávez, S., and A. Aguilera.** 1997. The yeast HPR1 gene has a functional role in transcriptional elongation that uncovers a novel source of genome instability. Genes Dev. **11:**3459–3470.
6. **Chávez, S., M. Garcia-Rubio, F. Prado, and A. Aguilera.** 2001. Hpr1 is preferentially required for transcription of either long or G+C-rich DNA sequences in *Saccharomyces cerevisiae*. Mol. Cell. Biol. **21:**7054–7064.
7. **Cheng, H., K. Dufu, C.-S. Lee, J. L. Hsu, A. Dias, and R. Reed.** 2006. Human mRNA export machinery recruited to the 5′ end of mRNA. Cell **127:**1389–1400.

8. **Dobson, M. J., R. E. Pearlman, A. Karaiskakis, B. Spyropoulos, and P. B. Moens.** 1994. Synaptonemal complex proteins: occurrence, epitope mapping and chromosome disjunction. J. Cell Sci. **107:**2749–2760.
9. **Durfee, T., M. A. Mancini, D. Jones, S. J. Elledge, and W. H. Lee.** 1994. The amino-terminal region of the retinoblastoma gene product binds a novel nuclear matrix protein that co-localizes to centers for RNA processing. J. Cell Biol. **127:**609–622.
10. **Fan, H. Y., R. J. Merker, and H. L. Klein.** 2001. High-copy-number expression of Sub2p, a member of the RNA helicase superfamily, suppresses *hpr1*-mediated genomic instability. Mol. Cell. Biol. **21:**5459–5470.
11. **Guo, S., M. A. Hakimi, D. Baillat, X. Chen, M. J. Farber, A. J. P. Klein-Szanto, N. S. Cooch, A. K. Godwin, and R. Shiekhattar.** 2005. Linking transcriptional elongation and messenger RNA export to metastatic breast cancers. Cancer Res. **65:**3011–3016.
12. **Huertas, P., and A. Aguilera.** 2003. Cotranscriptionally formed DNA:RNA hybrids mediate transcription elongation impairment and transcription-associated recombination. Mol. Cell **12:**711–721.
13. **Keene, J. D.** 2007. RNA regulons: coordination of post-transcriptional events. Nat. Rev. Genet. **8:**533–543.
14. **Kim, M., S. H. Ahn, N. J. Krogan, J. F. Greenblatt, and S. Buratowski.** 2004. Transitions in RNA polymerase II elongation complexes at the 3′ ends of genes. EMBO J. **23:**354–364.
15. **Kim, S., V. J. Bardwell, and D. Zarkower.** 2007. Cell type-autonomous and non-autonomous requirements for Dmrt1 in postnatal testis differentiation. Dev. Biol. **307:**314–327.
16. Reference deleted.
17. **Li, Y., A. W. Lin, X. Zhang, Y. Wang, X. Wang, and D. W. Goodrich.** 2007. Cancer cells and normal cells differ in their requirements for Thoc1. Cancer Res. **67:**6657–6664.
18. **Li, Y., X. Wang, X. Zhang, and D. W. Goodrich.** 2005. Human hHpr1/p84/Thoc1 regulates transcriptional elongation and physically links RNA polymerase II and RNA processing factors. Mol. Cell. Biol. **25:**4023–4033.
19. **MacLean, J. A., M. A. Chen, C. M. Wayne, S. R. Bruce, M. Rao, M. L. Meistrich, C. Macleod, and M. F. Wilkinson.** 2005. Rhox: a new homeobox gene cluster. Cell **120:**369–382.
20. **Marcon, E., and P. Moens.** 2003. MLH1p and MLH3p localize to precociously induced chiasmata of okadaic-acid-treated mouse spermatocytes. Genetics **165:**2283–2287.
21. **Masuda, S., R. Das, H. Cheng, E. Hurt, N. Dorman, and R. Reed.** 2005. Recruitment of the human TREX complex to mRNA during splicing. Genes Dev. **19:**1512–1517.
22. **Merker, R. J., and H. L. Klein.** 2002. *hpr1*Δ affects ribosomal DNA recombination and cell life span in *Saccharomyces cerevisiae*. Mol. Cell. Biol. **22:**421–429.
23. **Merz, C., H. Urlaub, C. L. Will, and R. Luhrmann.** 2007. Protein composition of human mRNPs spliced in vitro and differential requirements for mRNP protein recruitment. RNA **13:**116–128.
24. **Moens, P. B., N. K. Kolas, M. Tarsounas, E. Marcon, P. E. Cohen, and B. Spyropoulos.** 2002. The time course and chromosomal localization of recombination-related proteins at meiosis in the mouse are compatible with models that can resolve the early DNA-DNA interactions without reciprocal recombination. J. Cell Sci. **115:**1611–1622.
25. **Moore, M. J.** 2005. From birth to death: the complex lives of eukaryotic mRNAs. Science **309:**1514–1518.
26. **Nishimune, Y., and H. Tanaka.** 2006. Infertility caused by polymorphisms or mutations in spermatogenesis-specific genes. J. Androl. **27:**326–334.
27. **Rehwinkel, J., A. Herold, K. Gari, T. Kocher, M. Rode, F. L. Ciccarelli, M. Wilm, and E. Izaurralde.** 2004. Genome-wide analysis of mRNAs regulated by the THO complex in Drosophila melanogaster. Nat. Struct. Mol. Biol. **11:**558–566.
28. **Rodríguez-Trelles, F., R. Tarrio, and F. J. Ayala.** 2005. Is ectopic expression caused by deregulatory mutations or due to gene-regulation leaks with evolutionary potential? Bioessays **27:**592–601.
29. **Romanienko, P. J., and R. D. Camerini-Otero.** 2000. The mouse Spo11 gene is required for meiotic chromosome synapsis. Mol. Cell **6:**975–987.
30. **Rondón, A. G., S. Jimeno, M. Garcia-Rubio, and A. Aguilera.** 2003. Molecular evidence that the eukaryotic THO/TREX complex is required for efficient transcription elongation. J. Biol. Chem. **278:**39037–39043.
31. **Rulli, S. B., P. Ahtiainen, S. Makela, J. Toppari, M. Poutanen, and I. Huhtaniemi.** 2003. Elevated steroidogenesis, defective reproductive organs, and infertility in transgenic male mice overexpressing human chorionic gonadotropin. Endocrinology **144:**4980–4990.
32. **Rulli, S. B., and I. Huhtaniemi.** 2005. What have gonadotrophin overexpressing transgenic mice taught us about gonadal function? Reproduction **130:**283–291.
33. **Shanker, S., Z. Hu, and M. F. Wilkinson.** 2008. Epigenetic regulation and downstream targets of the *Rhox5* homeobox gene. Int. J. Androl. **31:**462–470.
34. **Sharpe, R. M., C. McKinnell, C. Kivlin, and J. S. Fisher.** 2003. Proliferation and functional maturation of Sertoli cells, and their relevance to disorders of testis function in adulthood. Reproduction **125:**769–784.
35. **Strässer, K., S. Masuda, P. Mason, J. Pfannstiel, M. Oppizzi, S. Rodriguez-Navarro, A. G. Rondon, A. Aguilera, K. Struhl, R. Reed, and E. Hurt.** 2002. TREX is a conserved complex coupling transcription with messenger RNA export. Nature **417:**304–308.
36. **Wang, X., Y. Chang, Y. Li, X. Zhang, and D. W. Goodrich.** 2006. Thoc1/Hpr1/p84 is essential for early embryonic development in the mouse. Mol. Cell. Biol. **26:**4362–4367.
37. **Wang, X., Y. Li, X. Zhang, and D. W. Goodrich.** 2007. An allelic series for studying the mouse Thoc1 gene. Genesis **45:**32–37.
38. **Wellinger, R. E., F. Prado, and A. Aguilera.** 2006. Replication fork progression is impaired by transcription in hyperrecombinant yeast cells lacking a functional THO complex. Mol. Cell. Biol. **26:**3327–3334.
39. **Wilhelm, B. T., S. Marguerat, S. Watt, F. Schubert, V. Wood, I. Goodhead, C. J. Penkett, J. Rogers, and J. Bahler.** 2008. Dynamic repertoire of a eukaryotic transcriptome surveyed at single-nucleotide resolution. Nature **453:**1239–1243.
40. **Zenklusen, D., P. Vinciguerra, J. C. Wyss, and F. Stutz.** 2002. Stable mRNP formation and export require cotranscriptional recruitment of the mRNA export factors Yra1p and Sub2p by Hpr1p. Mol. Cell. Biol. **22:**8241–8253.
41. Reference deleted.